Electrochemical Properties of Cu Deposition from Methanesulphonate Electrolytes for ULSI and MEMS Applications

Maksudul Hasan, Declan P. Casey and James F. Rohan

Tyndall National Institute, University College Cork, Lee Maltings, Cork, Ireland

Methanesulphonic acid (MSA) is an alternative to sulphuric acid electrolytes. The electrochemical nucleation and growth of Cu on a glassy carbon (GC) electrode was studied from the methanesulphonate and sulphate baths. The overpotential for Cu deposition was much smaller in the MSA bath compared to the traditional sulphuric acid bath. Cu nucleation occurred at a higher rate in the MSA bath. The measured diffusion coefficient value for Cu deposition from the MSA bath was 6.82×10^{-6} cm^2/s. The UV-Vis spectroscopic results confirmed that the coordination of Cu species was the same in both electrolytes. Cu electrodeposition on Ni sputtered Si substrate from the high efficiency MSA bath was found to be photoresist compatible with no void formation. 1D Cu nanorods were also deposited through AAO template on a Ni evaporated seed layer substrate showing potential applications as interconnects in ULSI and MEMS.

Introduction

Cu is the current and future interconnect material in high-end microprocessors and memory devices because of its lower electrical resistivity and higher electromigration resistance than aluminum. Dual damascene Cu electroplating is now commonly used in semiconductor devices usually employing a mixture of $CuSO_4/H_2SO_4$. To achieve a so-called bottom-up or super-conformal deposit, various types of organic additives are also added (1-2). Moreover, additives such as bis-(3-sodiumsulphopropyl disulphide) (SPS) that are used as accelerators decompose at Cu anodes influencing the gap-filling and the defect performance capability of Cu electroplating (3). The aging effect and the byproducts of polyethylene glycol (PEG) during copper electroplating have also been studied (4). PEG-Cl electrolyte that is commonly used as a suppressor in semiconductor Cu electroplating bath decomposes to PEG of smaller molecular weight at the cathode. The smaller molecular weight PEG is found to have less adsorption ability on the electrode surface, and thus the inhibiting effect on copper reduction decreases gradually.

In this study, we report methanesulphonic acid (MSA) is an alternative electrolyte system which could replace sulphuric acid in practical applications. MSA is a strong electrolyte and its conductivity in water is similar to other strong acids such as sulphuric or hydrochloric and higher than that of other organic acids (5). Nevertheless, MSA has a "green" character in two different ways. Firstly, it is odorless and does not generate toxic gas fumes which make it very safe to handle (5). Secondly, it is readily biodegradable and recyclable (6). Recycling of MSA is readily achieved because of its excellent solubility in water so that it can be extracted from an organic phase with small amounts of water. These result in easily treatable effluents that are less hazardous compared to all

other commercial baths such as sulphate, chloride, fluoride, etc. MSA also attract great attention because of its non-oxidant characteristics compared to other traditional electrolytes, i.e. sulphate, nitrates, etc. Additionally, MSA solutions are easy to handle since it remains in liquid form down to –60°C (H_2SO_4: 3°C) and it has a greater thermal stability than other organic acids. The baths produce a reduced amount of waste and sludge, and thus the early investment of resources can be minimized. Nevertheless, information on the fundamental properties of such electrolytes in the "open" scientific literature is very scarce. This paper will report the basic electrochemistry of Cu metal ion deposition in aqueous MSA solution by comparison with the traditional sulphate bath. Here, we will present electrodeposition of Cu on Ni sputtered Si substrate patterned using optical photolithography. We also report the fabrication of 1D Cu nanorods based on the anodized aluminum oxide (AAO) mediated direct electrodeposition technique from the MSA plating bath for interconnects in ULSI and MEMS applications.

Experimental

Cu methanesulphonate was prepared as follows. $Cu(OH)_2$ was first precipitated from the sulphate solution using NaOH (excess) accordingly the following equation:

$$CuSO_4.5H_2O + 2NaOH \rightarrow Cu(OH)_2 + Na_2SO_4 + 5H_2O \quad [1]$$

31.21 g (0.125 mol) of Cu sulphate pentahydrate (Fisher Scientific, analytical reagent grade) was dissolved in water and poured slowly in aqueous solution of sodium hydroxide (10 g, 0.25 mol) (Sigma-Aldrich, reagent grade, 97%). The bluish slurry Cu hydroxide was washed with deionised water (DI). The filtrate was dried in vacuo (1 mmHg) at 50 ^{0}C and used in the synthesis of Cu methanesulphonate. The reaction proceeds according to the following equation:

$$Cu(OH)_2 + 2CH_3SO_3H \rightarrow Cu(O_3SCH_3)_2.4H_2O + 2H_2O \quad [2]$$

The powdered Cu hydroxide (12.0 g, approx. 0.125 mol) was dissolved in MSA (24.025g, 0.250 mol) (Sigma-Aldrich, 99% anhydrous) at 80^{o}C for 1 hour, and enough deionised water (DI) was then added to produce a homogeneous solution. The formation of the Cu methanesulphonate was induced by isopropyl alcohol. The crystalline precipitate was collected by vacuum filtration and washed with isopropyl alcohol and ether. The solid product was brought to constant weight in vacuum (1 mmHg). The compound $Cu(O_3SCH_3)_2.4H_2O$ was characterised by EDTA complexometric titration, CHN analysis (Interscience Ce Instrument EA1110).

Cu deposition/dissolution experiments were carried out in a three electrode electrochemical cell. The working electrode glassy carbon (GC) was constructed from a 3 mm diameter vitreous carbon rod with an active surface area of 0.0803 cm^2 (geometrical area 0.07065 cm²). The electrode surface was polished successively with a 0.3, 0.1, and 0.05 μm alumina powder (Struers) to a mirror finish and was ultrasonically rinsed before the experiment. Two equal molar solutions for these experiments consisted of 0.05 M $CuSO_4.5H_2O$ (Fisher Scientific, analytical reagent grade) in 1 M H_2SO_4 (Air Products, 96 %) and 0.05 M $Cu(O_3SCH_3)_2.4H_2O$ (in house) in 1 M MSA (Sigma-Aldrich, 99 % anhydrous) were used. All electrochemical experiments were carried out with a CHI

660C potentiostat (CH Instruments Inc.) coupled to a personal computer, Ti/Pt mesh counter and H_2 reference electrode. The temperature of the cell was thermostatically controlled at 20 ± 1°C. Prior to a series of experiments, the electrolytic solution was deaerated for 2 hours with high-purity nitrogen, which was pre-saturated with water. The UV-Vis spectroscopy experiments of two equal molar solutions of 0.05 M $Cu(O_3SCH_3).4H_2O$ and $CuSO_4.5H_2O$ were carried out by the CARY 5000 spectrophotometer to compare the coordination of Cu^{2+} ions into solutions with the reference solutions of 1 M CH_3SO_3H and 1 M H_2SO_4, respectively.

Cu electrodeposition on Si substrates were carried out using a mask with arrays of (100 µm x 100 µm) features and a pitch of 400 µm. These features were patterned in Ni sputtered Si substrate by photolithographic technique. A 100 mm diameter Si wafer was used as substrate with thin layers of Ti (200 Å) and Ni (1000 Å) were physically deposited by sputtering process. Here, Ti layer improves the adhesion of Ni to the Si substrate which acts as the conducting seed layer. A 12 µm thick positive photoresist AZ 9260 was spun on the wafer exposed and developed in AZ 400k. The Cu was deposited in the developed photoresist mold from 0.1 M $Cu(O_3SCH_3)_2.4H_2O$ / 1 M CH_3SO_3H at 20 ± 1 ^oC, with Ti/Pt mesh as counter electrode. After the electroplating the resist was stripped in acetone; the wafer was then rinsed and dried with nitrogen. 1D nanoscale electrodeposition for interconnects in 3D integration of ULSI and MEMS application was performed on commercial anodized aluminium oxide (AAO) Anodisc membranes (Whatman, 10^9 pores per cm^2). The complete fabrication process of Cu nanorods is illustrated in Fig. 1. A 500 nm thin layer of Ni conducting layer was deposited onto one side of AAO template by e-beam evaporation technique (Temescal FC-2000). The electrodeposition was carried out in 0.24 M $Cu(O_3SCH_3)_2.4H_2O$ / 1.8 M CH_3SO_3H at 20 ± 1 ^oC with a slow convection of the electrolyte at a constant current 40 mA. In a two electrode set up a Ti/Pt mesh was the anode and Ni seed layer on the AAO substrate was the working electrode (cathode). A Cu wire was connected to the Ni conducting side of the template by silver conductive paint (Radionics Ltd. Ireland) and left to dry overnight before use. The morphology of the Cu deposits were analysed by scanning electron microscopy (SEM) (FEI Nova 630 Nano-SEM and Hitachi S-4000 at 15 kV) and characterised by X-ray powder diffraction (Phillips PW3710-MPD with Cu Kα radiation, l =1.54056 Å, at 40 kV (35 mA) and data was analysed using Philips X'pert XRD software).

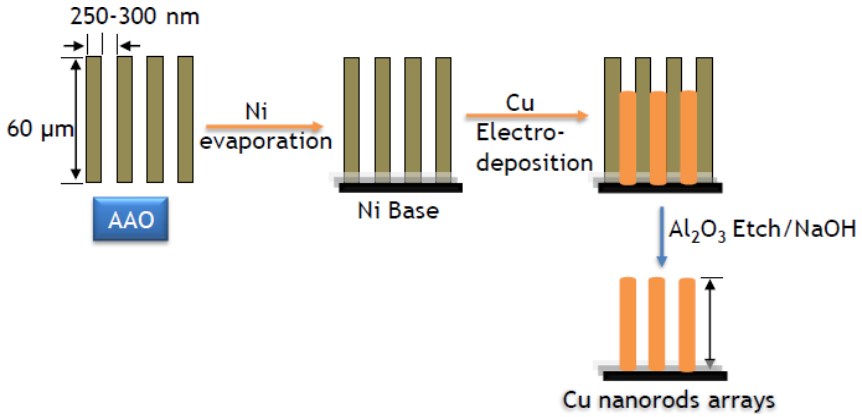

Figure 1. Schematic illustration of the synthesis process of the high aspect ratio Cu nanorod arrays.

Results and Discussion.

The electrochemical window of the background electrolyte of 1M aqueous methanesulphonic acid and sulphuric acid solutions (Fig. 2) in the cathodic direction was measured by cyclic voltammetry. The small current, which remains constant over the potential interval from 0 to –0.3 V, is not due to a Faradic process, but is merely a capacitive current associated with the action of a continuous potential change during the cyclic voltammetry experiment. On the other hand, the sharp current rise at –0.4 V is due to hydrogen evolution. Thermodynamically, hydrogen evolution on an electrode surface can occur starting from 0 V_{SHE}. In this case the overpotential of 0.3 V for hydrogen evolution reflects the activation barrier that has to be overcome for the formation of hydrogen gas on the GC electrode in the methanesulphonate bath. No electrochemical reaction on the GC electrode takes place at potentials more positive than –0.3 V.

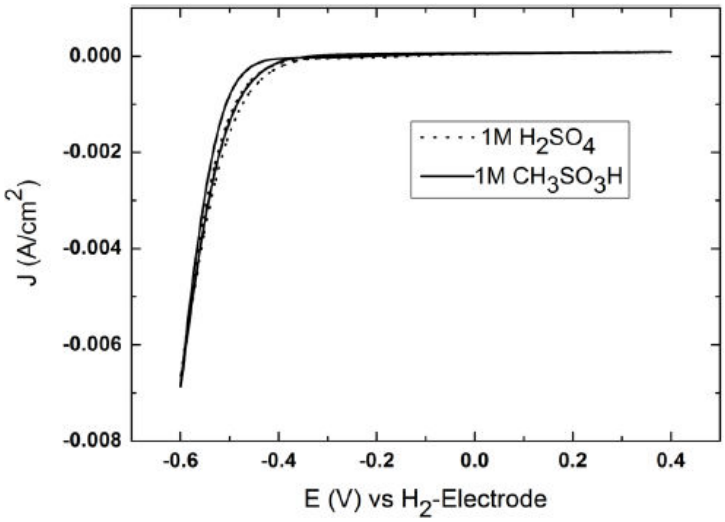

Figure 2. CVs of 1M CH_3SO_3H (solid line) and1M H_2SO_4 (dotted line) on a GC disc electrode (Conditioning/initial potential: 0.4 V, 20 s; scan rate: 0.01 V/s).

Fig. 3 (a) shows two cyclic voltammograms of the Cu deposition obtained from methanesulphonate and sulphate baths during the forward sweep to lower potentials. In methanesulphonate a sharp rise at around 0.125 V is observed by comparison with 0.05 V in sulphate bath that passes through a maximum at around 0 V corresponding to -0.160 V for sulphate bath, and then decreases due to the increase of the diffusion layer thickness. In the reversed sweep, the current passes through zero at around 0.275 V before oxidation commences. This crossover potential is a good approximation of the equilibrium potential. It is seen that the cathodic peak maximum is shifted by 0.160 V to a more positive potential values in methanesulphonate bath (full line) compared to the sulphate bath (dotted line), thus, the critical over-potential for Cu deposition on GC electrode is much lower in the methanesulphonate. In addition, the cathodic peak current (I_p = 0.019 A/cm^2) in methanesulphonate bath is also higher than that obtained in sulphate bath (Ip = 0.014 A/cm^2), implying that the amount of Cu deposit at the same potential interval and sweep rate is particularly higher in the methanesulphonate bath. The nucleation loops shown in Fig. 3 (b) are an indication of the nucleation and growth process of Cu on glassy carbon substrate. The initial adsorption and nucleation rate of Cu^{2+} ions at the cathode is faster

compared to that of in sulphate bath. Further on the reverse sweep, when $E > E_{eq}$ the anodic peak corresponding to the dissolution of Cu is observed.

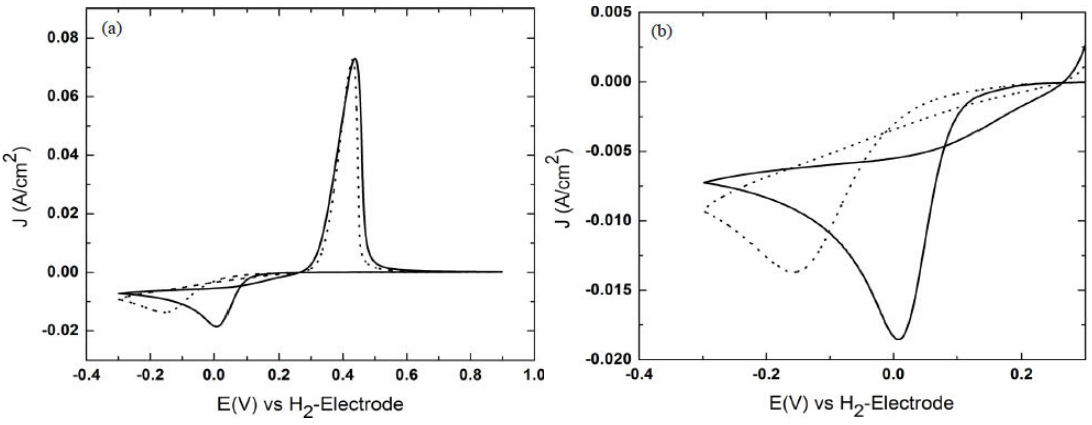

Figure 3. (a**)** CVs of Cu deposition from methanesulphonate (solid line) and sulphate (dotted line) bath on a GC disc electrode and (b) close-up view of the nucleation loops of copper deposition (Conditioning/initial potential: 0.4 V, 20 s; scan rate: 0.05 V/s).

Cyclic voltammetry is not always an accurate quantitative technique since the electrode potential and hence the kinetics for electrochemical reactions changes continuously during the time scales of the experiment (7). Therefore, the kinetics of Cu deposition was also investigated by chronoamperometric experiments. Two chronoamperometric current transients from methanesulphonate and sulphate baths are shown in Fig 4, in which the electrode potential was instantaneously changed from 0.4 V, (a value where no electrochemical activity occurs), to -0.1 V in the overpotential deposition region. Both the transients increase through a maximum and reach the same current value at longer times. This behaviour is expected when reduced species are not soluble into electrolytes. However, it can be seen from the Fig. 4 that at the same potential steps, the current transient in methanesulphonate bath is significantly steeper than the sulphate bath which represents a faster nucleation rate in this bath at similar potentials.

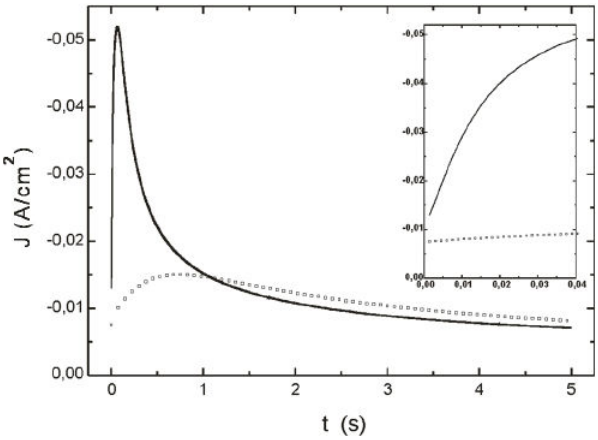

Figure 4. Chronoamperograms of Cu deposition from methanesulphonate (solid line) and sulphate (square line) bath at -0.1 V on a GC disc electrode (Conditioning/initial potential: 0.4 V, 10 s: deposition time 5 s) and the inset enlarged initial time region.

The determination of the diffusion coefficient of Cu^{2+} ions in the methanesulphonate bath is estimated using Cottrell equation (7).

$$I(t)=n.F.A.C.\left(\sqrt{\frac{D}{\pi t}}\right) \qquad [3]$$

in which n- the number of electrons transferred per molecule, F - the Faraday constant (96484.6 C/mol), A - the electrode area (cm^2), D - the diffusion coefficient (cm^2/s), and C - the concentration of the species in the solution (mol/cm^3). A potential step was applied to the GC electrode from an initial value of 0.4 V (where no electrochemical reaction occurs) to a final value of –0.125 V and held at this potential for 5 s. Afterwards, the copper deposit was removed by applying an anodic potential of 0.7 V for 30 s. The measured diffusion coefficient value of Cu^{2+} ions is found to be 6.82 x 10^{-6} cm^2/s (Slope = 1.421 x 10^{-2}, obtained from the initial part of the Cottrell plot {I/A vs. $\frac{1}{\sqrt{t}}$}, correlation coefficient value 0.99994). There is no literature available for the diffusion coefficient value of Cu^{2+} ions estimated from methanesulphonate bath to compare.

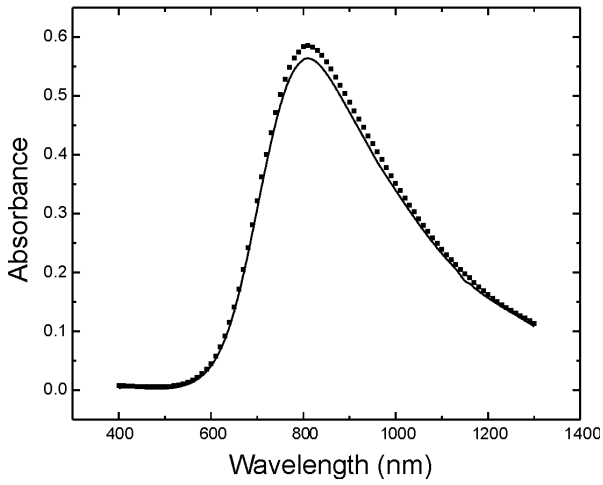

Figure 5. The absorbance as the function of wavelength (λ) in methanesulphonate (solid line) and in sulphate (filled square line) bath.

Fig. 5 shows UV-Vis spectrometry of two solutions, where the maximum of the absorption band in $CuSO_4.5H_2O$ solution is at 810 nm, and no shift of the maximum absorption is apparent in the $Cu(O_3SCH_3)_2.4H_2O$ solution. This indicates that the Cu species in both electrolytes have the same coordination with respect to surrounding anions and water molecules $[Cu(H_2O)_6]$. It can also be seen from Fig. 5 that the absorbance in $Cu(O_3SCH_3)_2.4H_2O$ solution is somewhat lower which can be attributed to weaker bond strength. This can be explained in terms of the electronic resonance effects which makes the sulphate ion more stabilised and therefore strong overlap with the vacant d orbital. On the other hand, the presence of larger CH_3- group instead of the O atom which has an electron donating effect in the methanesulphonate anion results in lower stabilisation and therefore, weaker overlap with the d orbitals. The high efficiency of the methanesulphonate bath can be interpreted, at least partially in terms of the methanesulphonate anion which acts as an accelerator added as the Cu salt itself.

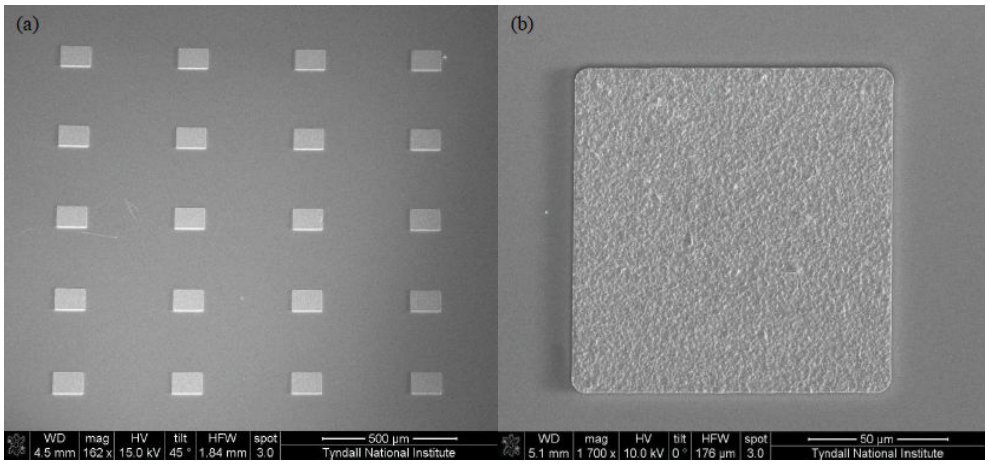

Figure 6. (a) SEM of Cu micro-pitch arrays in a 12 µm thick AZ 9260 photoresist mold after resist stripped, and (b) magnified single pitch showing linear square features with void free deposit.

Fig. 6(a) shows a Cu deposit array in a 12 µm thick AZ 9260 photoresist mold after photoresist removal. The experiment demonstrated the chemical stability of the photoresist in methanesulphonate bath and the Cu electrodeposition efficiency without additive influence. The Cu was deposited to fill the open structures at 10 mA/cm^2 for 1 hour. The uniformity of the deposited Cu from methanesulphonic acid electrolyte is shown in Fig. 6(b), it can also be seen that the dimension of the developed features are linear square size i.e., no side wall undercutting or voids are observed. Therefore, the photolithography assisted Cu interconnects fabrication is viable in methanesulphonic acid electrolyte.

It is well known that the properties of metallic films differ remarkably from the bulk materials when the thickness of the metallic films decreases to sub-micron or nano-scale length (8-9). Here, the electrical resistivity of Cu thin film is estimated using Four-Point Probe technique according to the following equation:

$$\rho = \frac{G(s,t)V}{I} \qquad [4]$$

Where, G is the geometric factor has a unit of lengths and given by the following equation (10):

$$G = t.{}^{\pi}/_{\ln(2)}.C\left({}^{d}/_{s}, {}^{a}/_{d}\right) \qquad [5]$$

Where, C is the additional correction factor due to finite dimension of the film, a and d are the length and breadth, s is the probe spacing. Fig. 7 shows the sheet resistance curve for which current and voltage are linearly proportional. Using the value of G suggested by F.M. Smits (10), the estimated sheet resistivity is 2.12 µΩ cm (G = 4.2209 for a = d, 10 mm and s = 10^{-3} m, here t = 1.02 x 10^{-6} m, slope = 0.00494 Ωm), the value is comparable with available literature data (11).

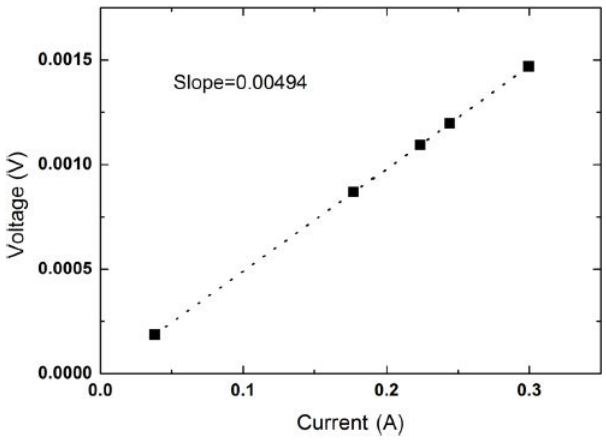

Figure 7. Sheet resistance curve for 1 x 1 cm^2 square size and 1.02 µm thick Cu film.

Fig. 8 (a) shows SEM image of well-ordered and homogeneous growth of Cu nanorod arrays from a bath of 0.24 M $Cu(O_3SCH_3)_2.4H_2O$ in 1.8 M CH_3SO_3H. The average diameter of the Cu nanorods is measured to be 290 nm which correlates with the value of pores diameter of the AAO template. The deposition rate is 0.55 µm/min at 40 mA with an additive-free solution. This compares with the slower deposition rate of 0.32 µm/min (12) for a Cu sulphate bath operated under the same conditions. Note that when the typical additives PEG and Cl^- were added to the MSA electrolyte the templated deposits were solid rather than the tubes achieved in the sulphate system described in reference (12). Thus it would appear that the suppression effects of that combination of additives do not govern the deposition type in the MSA bath and high rate solid structures are achieved. Indeed it may be that the MSA anion acts as an accelerator for Cu deposition and leads to the enhanced kinetics for deposition observed in the voltammetry and chronoamperometry. The XRD pattern reveals that Cu nanorods are polycrystalline having a preferred orientation of (111); the peaks from Ni seed layer are also apparent, see Fig. 8(b). It is well known that the preferred crystalline orientation of deposits depend on the conditions of electrodeposition such as current density, bath composition, electrolyte convection, temperature, pH etc. It has been observed that the increasing cathodic current from 40 mA to 100 mA or bath temperature from 20 to 40°C resulted in the development of (200) and (220) orientations, at the same pH (0.45).

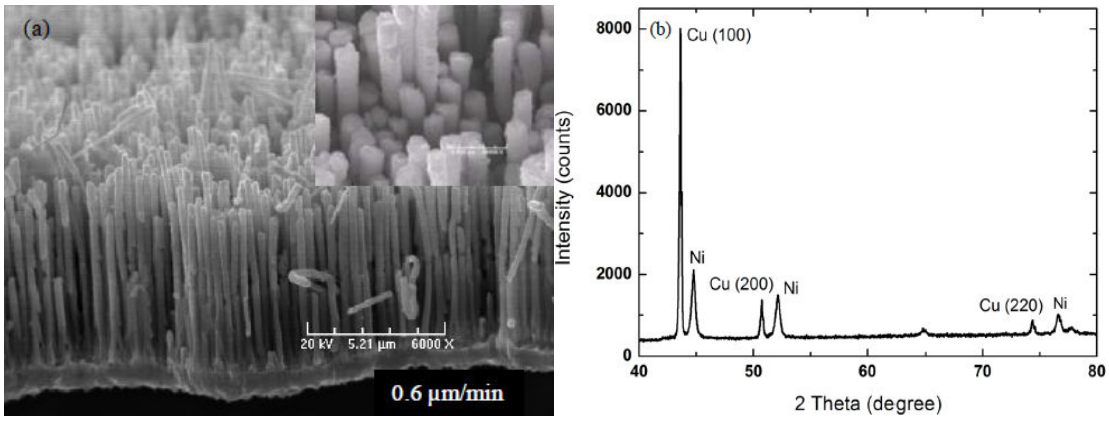

Figure 8. (a) SEM image of Cu nanorod arrays (inset is magnified view) and (b) XRD patterns of Cu deposit.

Conclusions.

Methanesulphonic acid has been shown to be a potential electrolyte for Cu electrodeposition. In this paper, we presented a preliminary study of Cu electrodeposition on the glassy carbon electrode from the methanesulphonic and sulphuric acid electrolytic solutions. The cyclic voltammetry results indicate that the overpotential for the Cu deposition is much lower in methanesulphonate bath. Consequently, from the current transients it is evident that for a fixed value of the overpotential, the kinetics of Cu nucleation is larger in the methanesulphonic acid bath by comparison with the sulphuric acid bath. The diffusion coefficient for the Cu deposition from methanesulphonic acid is estimated to be 6.82 x 10^{-6} cm^2/s. The difference in nucleation behaviour is most likely due to the difference in the adsorption of the background electrolyte ions and Cu^{2+} on the GC interface surface, where the coordination strength of Cu^{2+} ions with surrounding anions or water molecules influences the formation of a critical nucleus that precedes further growth. The enhanced kinetics and lower over-potential for the Cu electrodeposition using methanesulphonic acid may result from accelerator effects of the MSA by comparison with the sulphuric acid electrolyte.

Void free Cu deposits have also been fabricated by a through-mold electroplating process on Ni sputtered Si substrates. Cu square pads (100 μm x 100 μm) with a pitch of 400 μm has been demonstrated. The electrical resistivity of the as deposited Cu thin film is measured to be 2.12 μΩ cm which correlates with literature values for Cu from sulphate baths. Cu nanorods were also electrodeposited through an AAO template on Ni evaporated substrate to investigate sub micron deposition from the MSA bath. The Cu methanesulphonate bath is found to be suitable for high rate deposition of void free Cu micron scale pads and nanorod interconnects for ULSI and MEMS applications.

Acknowledgments.

Enterprise Ireland Technology Development Project CFTD/05/IT/317.

M. Hasan. KU Leuven M.Sc. Thesis "Electrochemical nucleation and growth of Cu from sulfuric and methanesulfonic acid solutions" under the direction of Prof. L. Heerman.

References.

1. T.P. Moffat, D. Wheeler, W.H. Huber and D. Josell, *Electrochem. Solid State Lett.*, **4**, C26 (2001).
2. L.T. Koh, G.Z. You, S.Y. Lim, C.Y. Lim and P.D. Foo, *Microelectron. J.*, **32**, 973 (2001).
3. S.-Y. Hu, C.-C. Hong and W.-H. Lee, "Investigation of bis-(3-sodiumsulphopropyl disulphide) (SPS) aging during deplating process on Pt contact pin", *abstract*, submitted in the 215th ESC meeting, 24-29 May, 2009, San Francisco, CA, USA.
4. C.-Y. Wu, W.-H. Lee, C.-T. Wu, and C.-C. Hong, "Investigation of the aging effect and the byproducts of polyethylene glycol during copper electroplating", *abstract*, submitted in the 215th ESC meeting, 24-29 May, 2009, San Francisco, CA, USA.
5. M. D. Gernon, M. Wu, T. Buszta and P. Janney, *Green Chem.*, **1**, 127 (1999).

6. J. Ma, Y. Kale and M. Turnbull, Biocatalysis/Biodegradation database, University of Minnesota (1997).
7. A.J. Bard and L.R Faulkner, *Electrochemical Methods. Fundamental and Applications*, p. 218, John Wiley and Sons, New York (1980).
8. M.D. Uchic, D.M. Dimiduk, J.N. Florando and W.D. Nix, *Science*, **305**, 986 (2004).
9. Z.P Bazant, Z.Y. Guo, H.D. Espinosa, Y. Zhu and B. Peng, *J. Appl. Phys.*, **97**, 073506 (2005).
10. F.M. Smits, Measurement of Sheet Resistivities with the Four-Point Probe, *The Bell System Technical Journal*, May 1958.
11. P. Dixit, C.W. Tan, L. Xu, n. Lyn, J. Miao, J.H.L. Pang, P. Backus and R. Preisser, *J. Micromech. Microeng.*, **17**, 1078 (2007).
12. T. Chowdhury, D.P. Casey and J.F. Rohan, *Electrochem. Commun.*, **11**, 1203 (2009).